J Musculoskelet Neuronal Interact 2006; 6(3):258-263

Original Article

Hylonome

Increased osteogenic response to exercise in metaphyseal versus diaphyseal cortical bone

M.W. Hamrick[1], J.G. Skedros[2], C. Pennington[1], P.L. McNeil[1]

[1]Department of Cellular Biology and Anatomy, Medical College of Georgia, Augusta, GA, USA;
[2]Department of Orthopaedics, University of Utah, Salt Lake City, Utah, USA

Abstract

Recent experimental data suggest that the anabolic response of bone to changes in physical activity and mechanical loading may vary among different skeletal elements, and even within different regions of the same bone. In order to better understand site-specific variation in bone modeling we used an experimental protocol in which locomotor activity was increased in laboratory mice with regular treadmill exercise for only 30 min/day. We predicted that the regular muscle contractions that occur during exercise would significantly increase cortical bone formation in these animals, and that the increase in cortical bone mass would vary between metaphyseal and diaphyseal regions. Cortical bone mass, density, and bone geometry were compared between these two regions using pQCT technology. Results indicate that exercise increases bone mineral content (BMC) in the mid-diaphysis by approximately 20%, whereas bone mass in the metaphyseal region is increased by approximately 35%. Endosteal and periosteal circumference at the midshaft are increased with exercise, whereas increased periosteal circumference is accompanied by marked endosteal contraction at the metaphysis, resulting in an increase in cortical area of more than 50%. These findings suggest that the osteogenic response of cortical bone to exercise varies significantly along the length of a bone, and more distal regions appear most likely to exhibit morphologic changes when loading conditions are altered.

Keywords: Bone Geometry, Bone Mineral Density, Mechanosensitivity, Bone Modeling

Introduction

The magnitude of peak stresses and strains developed in the limb skeleton during locomotion is an important consideration from the perspective of bone adaptation because strain magnitude is the principal transducing mechanism to which bone modeling is assigned in the "mechanostat" model[1-3]. We define bone modeling here as a gain in skeletal mass during growth via the addition and accretion of new tissue (after Skedros et al.)[4], as opposed to remodeling which involves the coupling of tissue resorption, formation, and reorganization (i.e., secondary osteon formation). Recent studies suggest that considerable heterogeneity exists in the response of bone to mechanical stimuli, not only among different skeletal elements but also among different regions within the same bone. In a recent study using the isolated rat ulna-loading model, Hsieh et al.[5] showed that the strain-related threshold for bone modeling differed significantly between three diaphyseal regions, even though these neighboring regions were only 3 mm apart (6 mm from proximal to distal). For example, the strain threshold varied from 1,343 microstrain proximally to 2,284 microstrain at mid-shaft to 3,074 microstrain distally. The strain threshold for bone modeling was largest distally, where locomotor bone strains are typically higher and smallest proximally where locomotor bone strains are lower. Other studies provide additional evidence for regional variation in the response of bone to both anabolic and catabolic stimuli. Iwamoto et al.[6] demonstrated that treadmill exercise in young rats produced a greater increase in cancellous bone mass at the distal tibia than at the proximal tibia, and the increase at the proximal tibia was greater than at the spine. Likewise, forelimb unloading in dogs produced greater bone loss in the third metacarpal than in the radius, and bone loss in the radius was greater than in the humerus[7].

The authors have no conflict of interest.

Corresponding author: Mark W. Hamrick, Department of Cellular Biology and Anatomy, Laney Walker Blvd. CB2915, Medical College of Georgia, Augusta, GA 30912, USA
E-mail: mhamrick@mail.mcg.edu

Accepted 17 April 2006

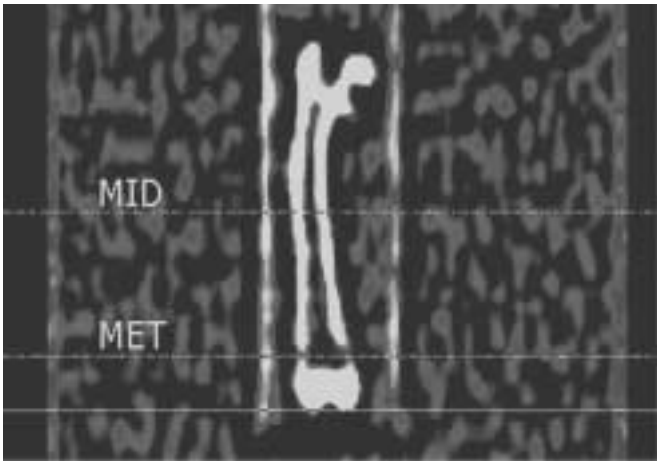

Figure 1. Norland Stratec pQCT scout view showing a mouse femur and the locations of two pQCT scans taken on each specimen, one at the midshaft (MID) and one across the distal metaphysis (MET).

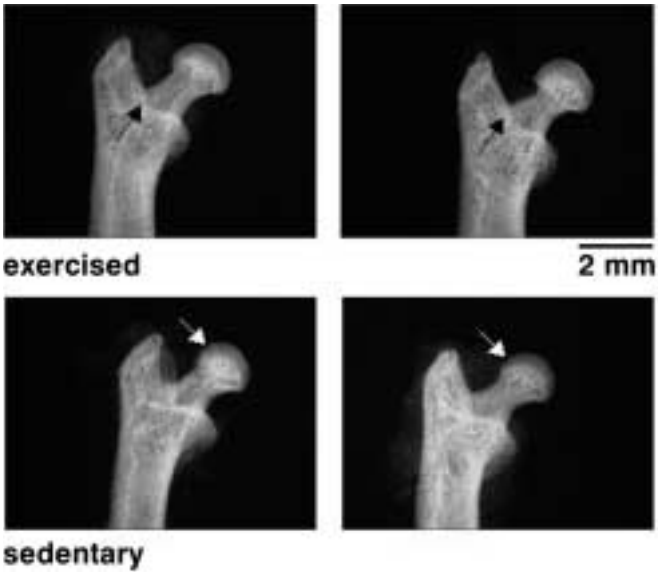

Figure 2. Faxitron radiographs of the proximal femur from exercised mice (top row) and sedentary mice (bottom row). Note the larger, more rounded femoral head in the exercised mice compared to the sedentary group, in which the superior aspect of the head is poorly developed (white arrows). Note also the more well-developed intertrochanteric crest in the exercised mice (black arrows).

In the metaphysis, trabeculae that develop via endochondral bone formation near the periphery of the growth plate coalesce and are incorporated into the cortical shell[8-9]. In contrast, cortical bone in the diaphysis develops primarily by intramembranous ossification. These developmental differences between metaphyseal and diaphyseal cortical bone may account for histologic differences that not only reflect

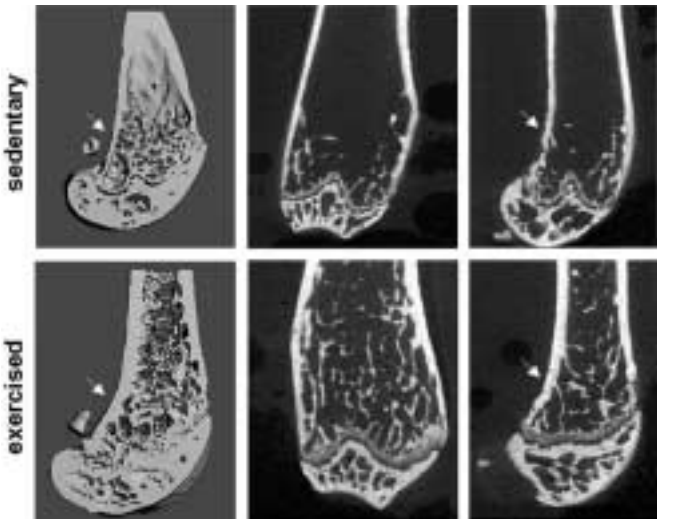

Figure 3. μCT images from the distal femur of a sedentary mouse (top) and exercised mouse (bottom) showing three-dimensional architecture of the metaphysis (left column), along with coronal (middle) and sagittal (right) sections through the same specimen. Note the thick cortical bone on the posterior aspect of the distal femur in the exercised mouse (arrow, bottom right) compared to the sedentary mouse (arrow, top right).

vascularity but also the lacuno-canalicular geometries that are deemed important in mediating mechanotransduction in bone tissue[10-12]. Thus, differences in the genetic regulation of growth and development, in addition to different epigenetic influences (e.g., tissue interactions involved in positional information), are likely to yield differences in mechanosensitivity between regions of a single bone[13-15]. We tested this prediction using an experimental design in which locomotor activity was increased in laboratory mice using treadmill exercise. We examined bone mineral content (BMC), bone mineral density (BMD), and bone geometry at two sites: the femur midshaft and distal femoral metaphysis.

Methods

Sample, exercise treatment and morphometry

Twenty-four female CD-1 mice were obtained from Charles River Laboratories (Wilmington, MA) at the age of 8 weeks and then habituated for one month in the animal housing facility at the Medical College of Georgia. Mice were randomly assigned to two treatment groups at 12 weeks of age: one group of 12 female mice began an exercise regimen that involved 30 minutes of treadmill exercise 5 days a week for 4 weeks, and another group was a sedentary cage-control group. Mice were exercised on a Columbus Instruments Exer-3/6 treadmill at a rate of 12 m/min. Exercised mice and sedentary control mice were sacrificed at the age of four months by CO_2 overdose as approved by the Medical

Parameter	Control (n=12)	Exercise (n=12)	P
Body mass (g)	31.5 (2.2)	30.0 (2.3)	ns
Femur length (mm)	18.5 (.30)	18.5 (.50)	ns
Femoral head diameter (a-p; mm)	1.59 (.04)	1.64 (.06)	<.05
Third trochanter diameter (m-l; mm)	1.98 (.10)	2.08 (.12)	<.05
Bicondylar diameter (mm)	2.97 (.12)	2.90 (.11)	ns
Iliopsoas mass (g)	0.12 (.01)	0.11 (.02)	ns
Quadriceps mass (g)	0.22 (.02)	0.23 (.03)	ns
Triceps surae mass (g)	0.16 (.01)	0.16 (.01)	ns

Table 1. Body mass, femoral dimensions, and hindimb muscle masses for the sedentary and exercised mice included for study. Means are shown with standard deviations in parentheses.

College of Georgia IACUC. Animals were collected at the age of four months because studies on inbred mouse strains indicate that mice reach peak bone density at this time[16]. Mice were weighed and the following muscles dissected free and weighed to the nearest .01 g: iliopsoas, quadriceps femoris, and triceps surae. Femora were dissected free, fixed in 10% formalin, and then stored in 70% ETOH for densitometry. Femur length, femoral head diameter, and transverse diameter across the third trochanter were measured using dial calipers.

Radiography and densitometry

Prior to densitometry, radiographs were taken of all femora at 3.0 kVP and 2.5 mA for 15s using a Faxitron X-ray cabinet. DEXA densitometry (PIXImus system) was used to measure whole-femur bone mineral content (BMC) and mineral density (BMD) from right femora. The PIXImus dual-energy X-ray absorptiometry system allows accurate measurement of bone mineral content and density from small lab animals using a relatively low X-ray energy (80/35 kVp) and high resolution (0.18 x 0.18 mm pixel size) to achieve contrast in low-density mouse bone. Replicability data indicate an excellent correlation (.99) between PIXImus BMC and total ashed weight. We used peripheral quantitative computed tomography (pQCT, Norland Stratec XCT-Research pQCT system) to analyze densitometric parameters from the femur midshaft and distal metaphysis (Figure 1). The pQCT technique is known to be a very useful and reliable approach for measuring trabecular and cortical bone area, mineral content, mineral density, and cross-sectional geometry in small rodent bones[17-20]. Cross-sections 1 mm thick were scanned at 4 mm/sec with a voxel size of 70 μm and a threshold value of 524.0 mg/cm^3 used to distinguish trabecular from (sub)cortical bone. Measurements collected from the midshaft cross-section include periosteal circumference, endosteal circumference, cortical area, total bone mineral content (BMC), total bone mineral density (BMD), and the polar area moment of inertia (J). The same measurements were calculated from the distal metaphyseal cross-section. Finally, we employed micro-computed tomography (μCT) in order to visualize the morphology of the trabecular network in the metaphyseal region of the femur. The specimens were scanned on a Scanco Medical CT40 system. For each specimen a length of approximately 5 mm was scanned at an isotropic voxel resolution of 12 microns. Images were acquired using cone-beam acquisition with an in-plane matrix size of 1,024 x 1,024 pixels and 1,000 projections over 360 degrees.

Statistical analysis

A single factor ANOVA with treatment (exercise or sedentary) as the factor was used to test for significant differences in the dependent variables described above. We also used a two-factor ANOVA with treatment (exercise vs. sedentary) and region (diaphysis vs. metaphysis) as the two factors to test for significant treatment*region differences in the response of bone densitometric and geometric variables (e.g., BMC, periosteal circumference) to exercise.

Results

The exercised and sedentary mice show no significant differences in body mass, femur length, or in the mass of individual hindlimb muscles (Table 1). The femoral head diameter is slightly larger in the exercised mice (Table 1), and radiographs show that the femoral head has a more rounded, globular shape in the exercised animals due to an expanded superior surface (Figure 2). Transverse diameter of the proximal femur across the third trochanter is also larger in the exercised mice (Table 1), due to expansion of the shaft in the direction of the gluteus maximus insertion, and the intertrochanteric crest is more well-developed (Figure 2). Whole-femur bone mineral content is significantly greater (20%) in the exercised mice, but whole-femur bone mineral density does not differ between groups (Table 2).

Parameter	Sedentary (n=12)	Exercised (n=12)	P
Whole-femur			
BMC (g)	0.031 (.003)	0.037 (.003)	<.001
BMD (g/cm^2)	0.070 (.007)	0.074 (.004)	ns
Midshaft			
BMC (mg/mm)	1.28 (.12)	1.52 (.13)	<.001
BMD (mg/cm^3)	768.8 (49.1)	775.7 (55.4)	ns
Distal Metaphysis			
BMC (mg/mm)	1.92 (.23)	2.57 (.31)	<.001
BMD (mg/cm^3)	488.4 (50.5)	558.5 (52.7)	<.01

Table 2. Bone densitometry data for the whole femur, midshaft, and distal femoral metaphysis. BMC=bone mineral content, BMD=bone mineral density. Means are shown with standard deviations in parentheses.

Parameter	Control (n=12)	Exercise (n=12)	P
Midshaft			
Periosteal circumference (mm)	4.55 (.17)	4.92 (.18)	<.001
Endosteal circumference (mm)	2.64 (.20)	2.95 (.24)	<.001
Cortical area (mm^2)	1.1 (.09)	1.24 (.10)	<.001
J (mm^4)	0.46 (.07)	0.59 (.07)	<.001
Metaphysis			
Periosteal circumference (mm)	7.0 (.25)	7.61 (.21)	<.001
Endosteal circumference (mm)	5.36 (.30)	4.99 (.47)	<.05
Cortical area (mm^2)	1.61 (.17)	2.60 (.44)	<.001
J (mm^4)	1.72 (.23)	3.33 (.64)	<.001

Table 3. Geometric properties of femora measured using pQCT sections taken across the midshaft and distal metaphysis. Means are shown with standard deviations in parentheses. J=polar area moment of inertia.

Similar results are obtained from pQCT slices taken across the femur midshaft, in which the exercised mice show approximately 20% higher BMC than sedentary mice but BMD does not differ between groups (Table 2).

A different pattern is observed at the metaphysis, where BMC is over 30% higher in the exercised mice and BMD is approximately 15% greater in the exercised mice (Table 2). It should, however, be noted here that pQCT underestimates BMD in cases where the cortical shell is thin, leading to an overestimation of differences in BMD between specimens that differ in cortical thickness[21]. Endosteal circumference is actually lower in exercised mice in the metaphyseal region, whereas the exercised mice have a higher endosteal circumference at the midshaft (Table 3). This is due to an increase in cortical area of over 50% at the metaphysis in the exercised mice, which accounts for the endosteal contraction (Table 3), whereas at the midshaft cortical area is increased by only 10% in exercised animals. μCT sections from the distal femur show that cortical bone thickness is increased dramatically in the metaphyseal region of the exercised animals compared to the sedentary mice (Figure 3). Two-factor ANOVAs reveal significant treatment x region interactions for endosteal circumference ($p<.001$), BMC ($p<.01$), BMD ($p<.05$), cortical area ($p<.001$), and the polar area moment of inertia ($p<.001$), confirming that the diaphyseal and metaphyseal regions differ significantly in their response to the exercise treatment.

Discussion

Exercise has far greater capacity to add new bone to the immature skeleton than to the skeleton of adults, and numerous studies in lab animals ranging from rats to dogs show that exercise produces little to no increase in bone mass among older, adult animals[22]. Our data from subadult mice are consistent with these earlier studies, and also with more recent work showing that jumping and climbing exercise increase bone formation and bone strength in the mouse hindlimb[23-24]. In the case of the mouse model used here, increased physical activity produced a slight but significant increase in the size of the femoral head and diameter of the third trochanter, and more marked increases in bone mineral content and cortical area at the distal femoral metaphysis. We recognize that analyses of changes in bone morphology in response to relatively simple exercise regimes, such as the experimental design utilized here, have their limitations. These have been clearly enumerated by Lovejoy et al.[25], and include the possibility that the sedentary animals represent a condition of disuse compared to the exercised animals, which may be more representative of the normal condition. However, our goal is to detect regional variation in the response of bone tissue to changes in physical activity, not to relate these responses to the magnitude of load and/or strain that the tissue experienced. Thus, we believe that regular exercise treatments are appropriate for investigating activity-related changes in bone modeling between different skeletal elements and different sites within the same bone.

Our finding that increased physical activity has a greater osteogenic effect in the distal femur than at the midshaft is consistent with previous work demonstrating regional variation in bone mechanosensitivity. It is likely that there are multiple mechanisms underlying this heterogeneity. Blood flow to the metaphyseal region of the femur in mice, rats, and dogs is 50-100% greater than blood flow to the femoral diaphysis[26-28]. Interstitial fluid pressure increases from proximal to distal regions of the limb, as does the response of bone tissue to anabolic and catabolic stimuli[29]. The extensive surface area provided by the trabecular lattice in metaphyseal regions also provides a greater area for bone-forming and -resorbing cells to attach and activate. As noted in the Introduction, trabeculae that develop via endochondral

bone formation near the periphery of the growth plate coalesce and are incorporated into the cortical shell. In contrast, cortical bone in the diaphysis develops primarily by intramembranous bone formation. Thus, differences in the genetic regulation of growth and development, in addition to different epigenetic influences, are likely to yield differences in mechanosensitivity between regions of a single bone[13-15,24].

Additional, important considerations that may also influence the response of metaphyseal bone to changes in physical activity are the biomechanical and metabolic influences of trabecular bone beneath the relatively thin cortex. Factors influencing the selective advantage of highly trabecular metaphyses in weight-bearing bones include the importance of preventing chondrosis by reducing stress concentrations, in addition to reducing tissue mass for optimizing locomotor energy efficiency[30]. Non-linear effects of functional loading (e.g., bending) on strain magnitudes and distributions, and hence interstitial and vascular fluid-flow dynamics, are also probably more pronounced toward the ends of a bone. This is supported by data showing that: 1) compared to the relative differences in failure strengths of cortical bone tested in tension, compression, and shear, trabecular bone is relatively weaker in shear[31-33], 2) the trabecular core can exhibit marked regional anisotropy within the same metaphyseal/epiphyseal region as the result of local variations in *architectural* parameters including trabecular orientation, thickness, connectivity, and/or apparent density[34-37], and 3) the relative contributions of cortical and trabecular bone to load-carrying capacity of a bone region can vary greatly over short distances within the same metaphyseal/epiphyseal region[38]. In turn, geometric cross-sectional properties of limb diaphyseal cortices based on standard engineering formulae (e.g., for calculating cross-sectional moments of area), which are commonly used to estimate strength and other structural properties of the shaft of a long bone, are highly inaccurate in regions where the trabecular bone core comprises greater than approximately 40% of the total cross-sectional area[39].

In view of the results of the present study, these considerations suggest that the development of site-specific differences in strain-related thresholds for bone modeling activity, especially between metaphyseal and diaphyseal regions, could be influenced by complex interactions between genetic, epigenetic, and extra-genetic stimuli. In turn, these factors can be variably correlated with the ultimate emergence of variations in the structural and material organization that can subsequently influence how the matrix deforms and fluid flows through different regions of a bone during functional loading. Clearly, the dose-response relationship between mechanical strains and osteogenesis is anything but simple[40-41]. Nevertheless, it is clear that the osteogenic response of cortical bone to exercise varies along the length of a bone, and more distal regions appear most likely to exhibit morphologic changes when loading conditions are altered.

Acknowledgements

We are grateful to Mr. Craig Byron for assistance in the lab, to Drs. Carlos Isales and Ding Xie for use of the PIXImus densitometer, and to Dr. Howard Winet who provided helpful insights and discussion. The pQCT data were collected by K. Grecco at the NEOUCOM, and we appreciate her help. Funding for this research was provided by the National Institutes of Health (NIAMS AR47655-01, AR049717-01).

References

1. Frost HM. The mechanostat: a proposed pathogenic mechanism of osteoporoses and the bone mass effects of mechanical and non-mechanical agents. Bone Miner 1987; 2:73-85.
2. Frost HM. Perspective: on our age-related bone loss: insights from a new paradigm. J Bone Min Res 1997; 12:1539-1546.
3. Frost HM. Changing concepts in skeletal physiology: Wolff's Law, the mechanostat, and the "Utah Paradigm". Am J Hum Biol 1998; 10:599-605.
4. Skedros JG, Mason MW, Bloebaum RD. Modeling and remodeling in a developing artiodactyl calcaneus: a model for evaluating Frost's mechanostat hypothesis and its corollaries. Anat Rec 2001; 263:167-185.
5. Hsieh Y-F, Robling A, Ambrosius W, Burr D, Turner C. Mechanical loading of diaphyseal bone *in vivo*: the strain threshold for an osteogenic response varies with location. J Bone Miner Res 2001; 16:2291-2297.
6. Iwamoto J, Yeh J, Aloia J. Differential effect of treadmill exercise on three cancellous bone sites in the young growing rat. Bone 1999; 24:163-169.
7. Jaworski Z, Liskova-Kiar M, Uthoff H. Effect of long-term immobilization on the pattern of bone loss in older dogs. J Bone Joint Surg Br 1980; 62B:104-110.
8. Enlow DH. Principles of Bone Remodeling: An Account of Post-natal Growth and Remodeling Processes in Long Bones and the Mandible. Thomas Springfield, IL; 1963.
9. Cadet E, Gafni R, McCarthy E, McCray D, Bacher J, Barnes K, Baron J. Mechanisms responsible for longitudinal growth of the cortex: coalescence of trabecular bone into cortical bone. J Bone Joint Surg Am 2002; 85:1739-1748.
10. Weinbaum S, Cowin SC, Zeng Y. A model for the excitation of osteocytes by mechanical loading-induced bone fluid shear stresses. J Biomech 1994; 27:339-360.
11. Qin L, Mak ATF, Cheng CW, Hung LK, Chan KM. Histomorphological study on pattern of fluid movement in cortical bone in goats. Anat Rec 1999; 255:380-387.
12. Palumbo C, Ferretti M, Marroti G. Osteocyte dendrogenesis in static and dynamic bone formation: an ultrastructural study. Anat Rec 2004; 278:474-480.
13. Judex S, Garman R, Squire M, Busa B, Donahue R, Rubin C. Genetically linked site-specificity of disuse osteoporosis. J Bone Miner Res 2004; 19:607-613.

14. Turner CH, Robling AG, Duncan RL, Burr DB. Do bone cells behave like a neuronal network? Calcif Tissue Int 2002; 70:435-442.
15. Skedros J, Grunander T, Hamrick M. Spatial distribution of osteocyte lacunae in equine radii and third metacarpals: considerations for cellular communication, microdamage detection, and metabolism. Cells Tissues Organs 2005; 180:215-236.
16. Beamer WG, Donahue LR, Rosen CJ, Baylink, DJ. Genetic variability in adult bone density among inbred strains of mice. Bone 1996; 18:397-403.
17. Ferretti JL. Perspectives of pQCT technology associated to biomechanical studies in skeletal research employing rat models. Bone 1995; 17(Suppl.):353S-364S.
18. Gasser JA. Assessing bone quantity by pQCT. Bone 1995; 17:145S-154S.
19. Hamrick MW, McPherron AC, Lovejoy CO. Bone mineral content and density in the humerus of myostatin-deficient mice. Calcif Tissue Int 2002; 71:63-68.
20. Hamrick MW. Increased bone mineral density in the femora of GDF8 knockout mice. Anat Rec 2003; 272A:388-391.
21. Brodt MD, Pelz GB, Taniguchi J, Silva MJ. Accuracy of peripheral quantitative computed tomography (pQCT) for assessing area and density of mouse cortical bone. Calcif Tissue Int 2003; 73:411-418.
22. Forwood M, Burr D. Physical activity and bone mass: exercises in futility? Bone Miner 1993; 21:89-112.
23. Kodama Y, Umemura Y, Nagasawa S, Beamer W, Donahue L, Rosen C, Baylink D, Farley J. Exercise and mechanical loading increase periosteal bone formation and whole bone strength in C57BL/6J mice but not in C3H/Hej mice. Calcif Tissue Int 2000; 66:298-306.
24. Mori T, Okimoto N, Sakai A, Okazaki O, Nakura N, Notomi T, Nakamu T. Climbing exercise increases bone mass and trabecular bone turnover through transient regulation of marrow osteogenic and osteoclastogenic potentials in mice. J Bone Miner 2003; 18:2002-2009.
25. Lovejoy CO, Meindl RS, Ohman JC, Heiple KG, White TD. The Maka femur and its bearing on the antiquity of human walking: applying contemporary concepts of morphogenesis to the human fossil record. Am J Phys Anthropol 2002; 119:97-133.
26. Humphreys E, Fisher G, Thorne M. The measurement of blood flow in mouse femur and its correlation with ^{239}Pu deposition. Calcif Tissue Res 1977; 23:141-145.
27. Kirkeby O, Berg-Larsen T. Regional blood flow and strontium-85 incorporation rate in the rat hindlimb skeleton. J Orthop Res 1981; 9:862-868.
28. Schnitzer J, McKinstry P, Light T, Ogden J. Quantitation of regional chondro-osseous circulation in canine tibia and femur. Am J Physiol 1982; 242:H365-375.
29. Turner CH. Site-specific skeletal effects of exercise: importance of interstitial fluid pressure. Bone 1999; 24:161-162.
30. Currey J. Bones: Structure & Mechanics. University Press, Princeton; 2002.
31. Keaveny TM, Hayes WC. Mechanical properties of cortical and trabecular bone. In: Hall BK (ed) Bone. CRC Press, Boca Raton; 1993:285-344.
32. Keaveny TM, Wachtel EF, Cutler MJ, Pinilla TP. Yield strains for bovine trabecular bone are isotropic but asymmetric. Trans Orthop Res Soc 1994; 19:428.
33. Ford CM, Keaveny TM. The dependence of shear failure properties of trabecular bone on apparent density and trabecular orientation. J Biomech 1996; 29:1309-1317.
34. Behrens JC, Walker PS, Shoji H. Variations in strength and structure of cancellous bone at the knee. J Biomech 1974; 7:201-207.
35. Brown TD, Ferguson AB. Mechanical property distribution in the cancellous bone of the human proximal femur. Acta Orthop Scand 1980; 51:429-437.
36. Goldstein SA. The mechanical properties of trabecular bone: dependence on anatomic location and function. J Biomech 1987; 20:1055-1061.
37. Goldstein SA, Goulet R, McCubbrey D. Measurement and significance of three-dimensional architecture to the mechanical integrity of trabecular bone. Calcif Tissue Int 1993; 53(Suppl.1):S127-S133.
38. Lotz JC, Cheal EJ, Hayes WC. Stress distributions within the proximal femur during gait and falls: implications for osteoporotic fracture. Osteoporos Int 1995; 5:252-261.
39. Ruff CB. The contribution of cancellous bone to long bone strength and rigidity. Am J Phys Anthropol 1983; 61:141-143.
40. Hsieh Y-F, Turner C. Effects of loading frequency on mechanically induced bone formation. J Bone Miner Res 2001; 16:918-924.
41. Fritton SP, Rubin CT. *In vivo* measurement of bone deformations using strain gauges. In: Cowin SC (ed) Bone Mechanics Handbook. CRC Press, Boca Raton; 2001:8.1-8.41.